Influence of the thermosphere on electromagnetic waves propagation: Application to GPS signal

Jean Lilensten, Philippe Delorme, Sophie Samouillan, Elodie Engel, Mathieu Barthelemy

Influence of the thermosphere on electromagnetic waves propagation: Application to GPS signal

Jean Lilensten, Philippe Delorme, Sophie Samouillan, Elodie Engel, and Mathieu Barthélémy

Laboratoire de Planetologie de Grenoble, Batiment D de Physique, Grenoble, France

Received 4 March 2004; revised 27 October 2004; accepted 17 November 2004; published 5 April 2005.

[1] We develop a model of wave propagation through the upper atmosphere taking into account the thermospheric collision frequencies and the Faraday rotation. We use this model to numerically test the effect of these collisions on the Global Positioning System (GPS) signal between 50 and 1000 km altitude. We study several characteristics of the GPS wave: ionospheric delay, dephasing, and variation of amplitude. We point out that the thermosphere influence is negligible, about 10^{-9} m on ionospheric delay, and may be considered as negligible on shorter-frequency waves. This study is extended to satellite-to-satellite communications both for quiet and magnetic storm cases. In this case the influence on the wave is greater but remains very weak.

Citation: Lilensten, J., P. Delorme, S. Samouillan, E. Engel, and M. Barthélémy (2005), Influence of the thermosphere on electromagnetic waves propagation: Application to GPS signal, *Radio Sci.*, *40*, RS2005, doi:10.1029/2004RS003057.

1. Introduction

[2] The ionosphere is generally considered as the only part of the upper atmosphere to affect electromagnetic waves. Nevertheless, according to *Brasseur and Solomon* [1984], the thermosphere has an effect on waves of a few MHz frequency particularly because of the collisions between the electrons of ionosphere and the neutral particles of thermosphere. The main influence is a heavy damping of the signal at these frequencies. This property has only been studied in the ionospheric D region, because the wave was reflected on the E layer. Nowadays, the signals emitted by spacecrafts such as the GPS system ones go trough the whole atmosphere. This system needs a very accurate precision which makes it necessary to obtain the best knowledge of the wave's perturbations.

[3] Two main topics may be influenced by the thermospheric GPS perturbations. The first one is the positioning. It is not expected from a rapid collision frequency consideration that the thermosphere influences the measured position by a large factor. However, some new applications of the positioning system such as dam or volcano survey require precisions of the order of the millimeter. It is not unrealistic to think that future applications could require even better accuracies. It is therefore important to reconsider the impact of the thermosphere with the help of the up-to-date thermospheric models.

[4] The second issue is space weather. Space weather aims at predicting and quantifying the solar activity and all its consequences on our space environment. It requires global real-time measurements. Beside other instruments, positioning network system is able to reach these constraints. It gives access to the total electron content (TEC) along the line of sight [*Mannucci et al.*, 1998, and references therein]. Currently, the expected accuracy of the TEC measurement is 2 TECU (1 TECU = 10^{16} electrons m^{-2}). Again, this accuracy will certainly drop in the future, and the influence of the thermosphere is then worth to be studied. Therefore we have endeavored to work out the influence of ionosphere-thermosphere coupling on GPS signal, both in matter of positioning and in matter of TEC assessment.

2. Theoretical Development

[5] Thermosphere cannot directly influence the wave propagation because a neutral medium is transparent to electromagnetic waves, but thermosphere has an indirect influence because of its permanent interaction with the charged medium of ionosphere. Their main coupling is the collisions between neutrals and ions or electrons. These collisions are one of the factors entering the expression of the refractive index. The refractive index enters in the computation of several parameters of GPS wave propagation: optical path delay, wave dephasing

0048-6604/05/2004RS003057

and wave amplitude. The polarization, which changes because of the Faraday rotation due to the Earth's magnetic field will not be studied here since it does not depend on the thermosphere-ionosphere coupling.

2.1. Propagation Equations

2.1.1. Refractive Index

[6] The GPS satellites send signals on two carrier frequencies. The L1 carrier is 1575.42 MHz (wavelength 19 cm) and carries both the status message and a pseudo-random code for timing. The L2 carrier is 1227.60 MHz (wavelength 24.4 cm) and is used for the more precise military pseudo-random code. We call f_{GPS} the GPS frequency and ω_{GPS} its pulsation. The following developments are indexed GPS, but are valid for any electromagnetic radio wave frequency. The detailed calculation of the refractive index n(r) at altitude r is given in Appendices A and B. In a collisional atmosphere it writes:

$$n(r) = \sqrt{1 - \frac{\omega_P^2/\omega_{GPS}^2}{1 - j(\nu(r)/\omega_{GPS} + \omega_B/\omega_{GPS}\rho\cos\vartheta)}}, \quad (1)$$

where ν(r) represents the total electron to ion and neutral collision frequency. Here θ is the angle between the nadir and the pointing direction as seen from the spacecraft. ρ is the ratio between the two perpendicular polarization fields E_y and E_x. ω_p(r) is the plasma pulsation which depends on the electron density n_e(r), the electron mass m_e and the permittivity of the medium (ε_o = 8,854 10^{-12} $F\ m^{-1}$):

$$\omega_P(r) = \sqrt{\frac{e^2 n_e(r)}{m_e \varepsilon_0}}. \quad (2)$$

When the pulsation is in Hz and the density in m^{-3}, we obtain:

$$\omega_P = 57.2\sqrt{n_e(r)}, \quad (3)$$

where ω_B is the gyropulsation. In a magnetic field of intensity B, its value is:

$$\omega_B = \frac{eB}{m_e}, \quad (4)$$

where m_e represents the mass of the electron.

[7] If we let Ψ be the angle between the electromagnetic vector $\vec{E}$ and the x axis, we can write its variation with the altitude z as:

$$\frac{d\Psi}{dz} = \omega_B \frac{1}{2c} \frac{\omega_P^2}{\omega_{GPS}\sqrt{\omega_{GPS}^2 - \omega_P^2}}, \quad (5)$$

where c is the speed of light. Then, ρ is simply equal to tan Ψ where the angle is computed from:

$$\Psi \approx \sum \frac{d\Psi}{dz} dz. \quad (6)$$

The rotation of Ψ is known as the Faraday rotation. It depends linearly on the gyropulsation and therefore on the B value. In the following, it will be shown that this rotation remains small compared to the collisions. The magnetic field varies with latitude and with altitude. However, its variation does not reach the order of magnitude. Taking the B variation into account does not affect the present conclusions. Moreover, we take here an upper value of B (0.5 G), which gives an upper limit to the Faraday rotation effect. Therefore we neglect the variation of B versus the altitude.

[8] In the following, we let $\bar{\nu}$ be the imaginary part of the denominator of the refractive index in equation (1):

$$\overline{\nu} = \frac{1}{\omega_{GPS}} \{\nu(r) + \omega_B \rho \cos\theta\}. \quad (7)$$

When the collisions and the magnetic field effect are neglected, we retrieve the "classical" refractive index formulation $n(r) = \sqrt{1 - \frac{\omega_P^2}{\omega^2}}$. In the general case, the refractive index is a complex number n(r) = $n_\Re$(r) + j $n_\Im$(r) where $n_\Re$(r) is the real part and $n_\Im$(r) the imaginary part. We set:

$$\begin{cases} \alpha(\omega_{GPS}, r) = \dfrac{\omega_{GPS}^4 + \omega_{GPS}^2\overline{\nu}^2(r) - \omega_{GPS}^2\omega_P^2(r)}{\omega_{GPS}^4 + \omega_{GPS}^2\overline{\nu}^2(r)} \\ \beta(\omega_{GPS}, r) = -\dfrac{\omega_{GPS}\omega_P^2(r)\overline{\nu}(r)}{\omega_{GPS}^4 + \omega_{GPS}^2\overline{\nu}^2(r)} \end{cases}, \quad (8)$$

Where α et β are respectively the real and the imaginary parts of n^2(r). After some algebra it comes:

$$\begin{cases} n_\Re(\omega_{GPS}, r) = \sqrt{\dfrac{1}{2}\left[\alpha(\omega_{GPS}, r) + \sqrt{\alpha^2(\omega_{GPS}, r) + \beta^2(\omega_{GPS}, r)}\right]} \\ n_\Im(\omega_{GPS}, r) = \dfrac{\beta(\omega_{GPS}, r)}{2n_\Re(\omega_{GPS}, r)} \end{cases}. \quad (9)$$

2.1.2. Influence on the Wave

[9] We use the plane wave approximation

$$\vec{E}(\vec{r}) = \vec{E}_0 e^{j\left(-\vec{k}\vec{r} + \omega_{GPS}t\right)}. \quad (10)$$

We set $\overline{\omega}_{GPS} = \frac{\omega_{GPS}}{c}$. Inserting (9) in (10), the phase (no unit) and amplitude (no unit) become:

$$\begin{cases} A(\omega_{GPS}, r) = e^{n_\Im(\omega_{GPS}, r)\overline{\omega}_{GPS} r} \\ \varphi(\omega_{GPS}, r) = \omega_{GPS} t - n_\Re(\omega_{GPS}, r)\overline{\omega}_{GPS} r \end{cases}. \quad (11)$$

Table 1. Electron-Neutral Collision Frequencies[a]

Molecule	Collision Frequency, collisions s^{-1}
N2	$2.33\ 10^{-11}$ n(N2) (1 − $1.2\ 10^{-4}$ Te) Te
O2	$1.8\ 10^{-10}$ n(O2) (1 + 0.036 $Te^{1/2}$) $Te^{1/2}$
O	$8.2\ 10^{-10}$ n(O) $Te^{1/2}$
H	$4.5\ 10^{-9}$ n(H) (1 − $1.35\ 10^{-4}$ Te) $Te^{1/2}$
He	$4.6\ 10^{-10}$ n(He) $Te^{1/2}$

[a]From *Schunk and Nagy* [2000]. Te is the electron temperature in Kelvin, and n(X) is the density of the molecule X in molecules cm^{-3}.

The most important parameter for GPS accuracy is the optical path r_{opt} (in meters):

$$r_{opt} = \int_P^S n(r)dr. \tag{12}$$

The difference of optical path between collisional plasma and collisionless plasma is:

$$\Delta r_{opt} = \int_P^S n(r)dr - \int_P^S n_{\Re}(\omega_{GPS}, r)dr. \tag{13}$$

We calculate the influence of collision on phase and amplitude in a similar way. Finally, the damping is defined as being 1, the amplitude variation (no unit).

2.1.3. Total Electron Content

[10] The second application of our calculation is the estimate of the total electron content. It can be computed through 2 different ways. First, using a limited development at second order of n (see Appendix C), we have:

$$\Delta R = \int_P^S (n-1)dr = \int_P^S \frac{n_e(r)e^2}{8\pi^2\varepsilon_0 Mf^2} \cdot dr = \frac{e^2}{8\pi^2\varepsilon_0 Mf^2}\int_P^S n_e(r)dr. \tag{14}$$

[11] The total electron content along the vertical is the projection of the electron density along the line of sight. Since the atmosphere is spherically stratified, it is necessary to use a Chapman function instead of a simple cosine law [*Smith and Smith*, 1972]:

$$TEC = \int_S^P n_e(r)drChap(\xi), \tag{15}$$

where ξ is the satellite zenith angle. If this angle is considered as constant along the vertical (i.e., if the spacecraft is high enough), we obtain:

$$TEC = \frac{8\pi^2 m_e f^2 \pi^2 \varepsilon_0 Chap(\xi)\Delta R}{e^2}. \tag{16}$$

However, we can also use the Faraday rotation (equation (5)) where we use equation (2) to relate Ψ to the electron density. From equation (3), one sees that the integral of the faraday rotation is directly a function of the total electron content. The integration gives [*Safaeinili et al.*, 2003]:

$$\Psi = 9.33 \times 10^5 \frac{B}{\omega_{GPS}} TEC. \tag{17}$$

2.2. Inputs

[12] Since we aim at studying the effects of the collisional thermosphere on the wave, we consider that the highest altitude of our model is 1000 km. At higher altitude, the collisions are negligible. Then, the total electron content (which is usually measured between 22 200 km and the ground) is called "ionospheric TEC," or iTEC to specify that the upper integration altitude is lower than usual [*Reinisch and Huang*, 1982, 1983; *Huang and Reinisch*, 1982]. To stress that it includes only the electrons below 1000 km, we note it $iTEC_{1000}$ in the following, as we have already made in our previous studies [*Lilensten and Blelly*, 2002; *Lilensten and Cander*, 2003].

[13] In order to get rid of the altitude dependence of the Chapman function in (16), we consider a GPS spacecraft upright the GPS receptor. Then, the Chapman term disappears in equation (16). This does not affect the order of magnitude of results. We make our simulation at middle latitude (45°N, 3°E, above the city of Grenoble) on 28 August. We choose active solar conditions (F10.7 = 253) in order to maximize the possible effect of the thermosphere.

[14] We need both a model of ionosphere and a model of thermosphere. For the ionosphere we used IRI2001, International Reference for Ionosphere [*Bilitza*, 2001]. The thermosphere is given by MSIS-E [*Hedin*, 1991]. In the E and *F* regions, the collision frequencies are from *Schunk and Nagy* [2000]. They are given in Table 1.

[15] Between 50 and 65 km we use the model from *Delcourt* [2003] using pressure instead of neutral density at these altitudes because of the low electron density and the high neutral density:

$$\nu = pressure \times 0.65 \times 10^6. \tag{18}$$

Finally, we take the electron-ions collisions ν_{ei} into account, from *Schunk and Nagy* [2000]. For single charged ions, it is:

$$\nu_{ei} = 54.5 \frac{n_i}{T_e^{3/2}}, \tag{19}$$

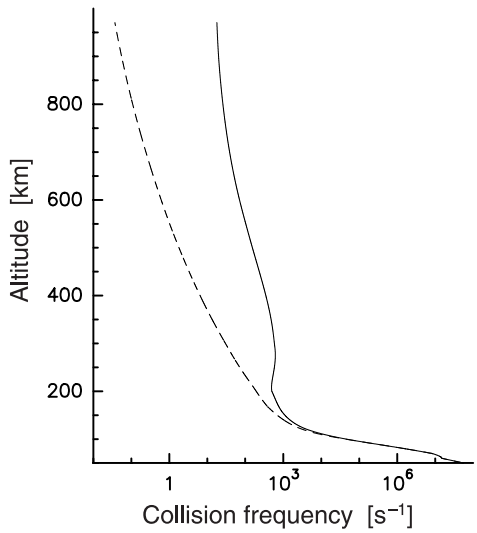

Figure 1. Collision frequency versus altitude. The dashed lines is the results without electron-ion collisions, i.e., with the parameters given in Table 1. The full line includes the electron-ion collisions ν_{ei} (equation (19)).

where n_i is the ion density in cm^{-3}. Its effect is important above about 200 km. The collision frequencies are shown in Figure 1.

2.3. Model Validation

[16] Equations (16) and (17) allow to retrieve the $iTEC_{1000}$ from the computation of the refractive index which depends on the electron density through the plasma pulsation or from the Faraday rotation. This electron density is given by a model and is used as input in our computations. Therefore, comparing our results with the direct integration of the electron density gives an independent way to validate the model and gives hints on the best way to deduce the total electron content from measurements. This comparison is shown in Figure 2. The value of the $iTEC_{1000}$ is 26 TECU. The two models fit well, with a difference lower than 1% of $iTEC_{1000}$ whatever the altitude, which is a good validation of our calculation.

3. Case of Satellite to Ground Communications

[17] The influence of the collisions on the wave can be explored on the ionospheric delay, on the dephasing and on the damping. The differences between the collisional and collisionless cases versus altitude (lower than 1000 km) are given in Table 2. The maximum on the ionospheric delay is about 4 angstroms. The variation on the dephasing is lower than 10^{-11}. The wave amplitude is decreased of 30 for one billion. All these are totally negligible.

[18] About 99% of the influence on ionospheric delay and dephasing is related to the D region. These parameters depend far more on neutral density than on electron density. However, damping variations are equally divided between the D region and the upper ionosphere. There is a remarkable influence of electron density through the F2 maximum of electron density that is responsible for the second increase of damping around 300 km.

[19] We have also explored the difference between the collisional atmosphere $iTEC_{1000}$ and the collisionless one. Again, the difference lays mostly in the D region, and is very weak. Indeed the whole variation throughout the ionosphere is lower than $1.2\ 10^{-9}$ TECU while the $iTEC_{1000}$ is 26 TECU. Therefore the thermosphere cannot influence the TEC measurement by mean of positioning systems.

[20] We have explored the influence of different parameters. The solar activity variation makes the collision frequency to vary mostly above 200 km, where the influence of the thermosphere on the wave propagation is small. Therefore increasing (or decreasing) the solar index gives no noticeable variation of our results. With a F10.7 index of 75, the differences are typically divided by a factor of about two, staying totally negligible.

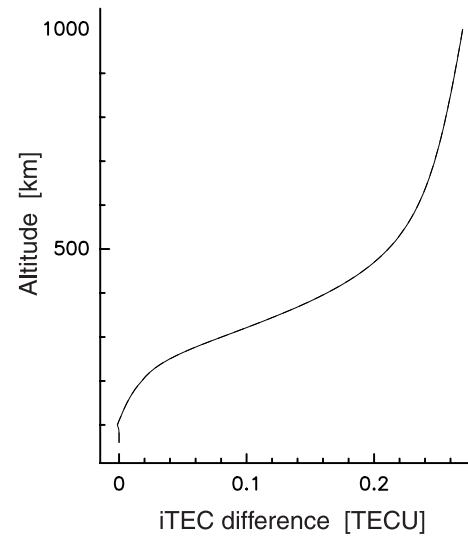

Figure 2. Difference between the $iTEC_{1000}$ deduced from the ionospheric profiler (IRI2001) and the actual computations from the optical path delay of GPS waves in the case of high solar activity (28 August 1999; see text). TECU stands for TEC unit (10^{16} e^- m^{-2}).

Table 2. Variation of the Delay, Phase, and Amplitude of the GPS Wave[a]

	Delay Variation, m	Phase Variation	Amplitude Variation
Collision only	$3.39269\ 10^{-10}$	$8.7237\ 10^{-12}$	0.9999999745
Full index	$3.39393\ 10^{-10}$	$8.7268\ 10^{-12}$	0.9999999583

[a]"Full index" refers to equation (1); "collision only" refers to the same formula where the rotation part has been neglected.

[21] The variation of the solar zenith angle does not change the magnitude of the collisional to collisionless difference on any parameter. In detail, the difference on the damping is twice as large at 1200 LT than at 1800 LT, while phase and ionospheric delay remain almost constant. This is a new clue of the strong dependence of damping on electron density at high altitude, which is quite affected by the position of the Sun in the sky.

[22] The cos(θ) term in equation (1) represents the Faraday rotation. We have studied its influence on the wave propagation. It is totally negligible on the optical path, since it accounts for only about 10^{-4} in the delay variation. Although it is also quite negligible on the damping, its behavior merits some comments (Figure 3). At low altitude, its influence is null up to about 200 km. The electron density is directly linked to its derivative. Therefore the *F* region electron peak corresponds to and inflexion point, which is visible in the figure around 270 km. At high altitude (above about 600 km), its influence is around 1/3 of the total damping.

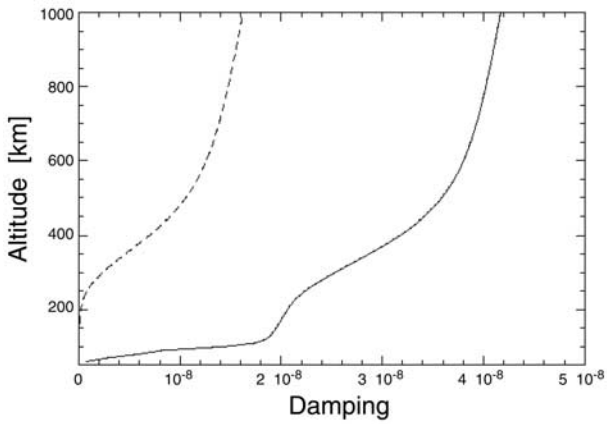

Figure 3. Height profiles of the damping (no unit) of the GPS wave through the atmosphere between 0 and 1000 km. The dashed line represents the damping when only the Faraday rotation is taken into account. The full line represents the total damping, i.e., due to Faraday rotation and collisions. A damping equal to 1 means that the wave is totally absorbed.

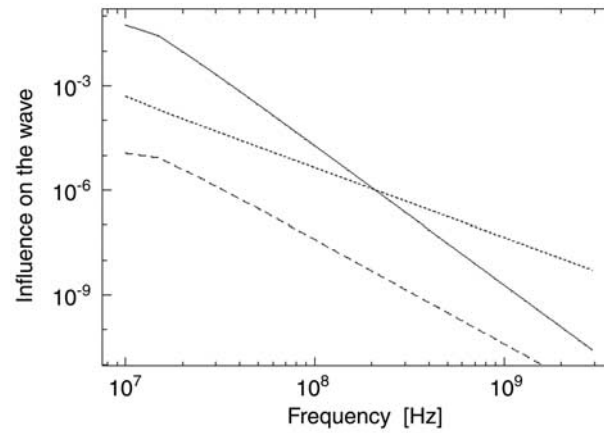

Figure 4. Influence of the collisions on the different wave parameters versus the frequency of the wave in the case of high solar activity: dephasing (radian) is shown by the dashed line, ionospheric delay (m) is shown by the full line, and damping is shown by the dotted line. A damping equal to 1 means that the wave is totally absorbed.

[23] Finally, we have extended our study to other wavelengths. The lower frequency that allows to cross the ionosphere is the plasma frequency, around 10 MHz. We choose 3 GHZ as the upper boundary, well above the GPS frequency. The results are shown in Figure 4. We note the existence of a slope rupture around 15 MHz for the variations of phase and of ionospheric delay. This is due to the fact that the wave has then a frequency lower than the collision frequency. Damping does not have any slope fracture because it does not depend only on the real part of the refractive index. Besides, we notice that these three parameters have a different sensitivity to the frequency: the damping variation is 5 decades, dephasing variation is 7 decades and ionospheric delay variation is 9 decades. Thus, if the phase and damping are negligible whatever the frequency, at 10 MHz the ionospheric delay is 10 cm and cannot be neglected anymore.

4. Case of Satellite-to-Satellite Communications

[24] The satellite-to-satellite communications are becoming more common. The geometry is shown in Figure 5. We consider two satellites in the equatorial plane communicating with each other from the morning side to the evening side. Noon is at the middle, so that the satellite angle is simply the longitude. The wave crosses the whole atmosphere with a lowest altitude of 50 km at noon. Then, the two angles between the Sun-Earth line and the spacecrafts is ±30°. Because of the low latitude, the hmF2 altitude stands at about 400 km height, while it would be at lower elevation at auroral latitudes.

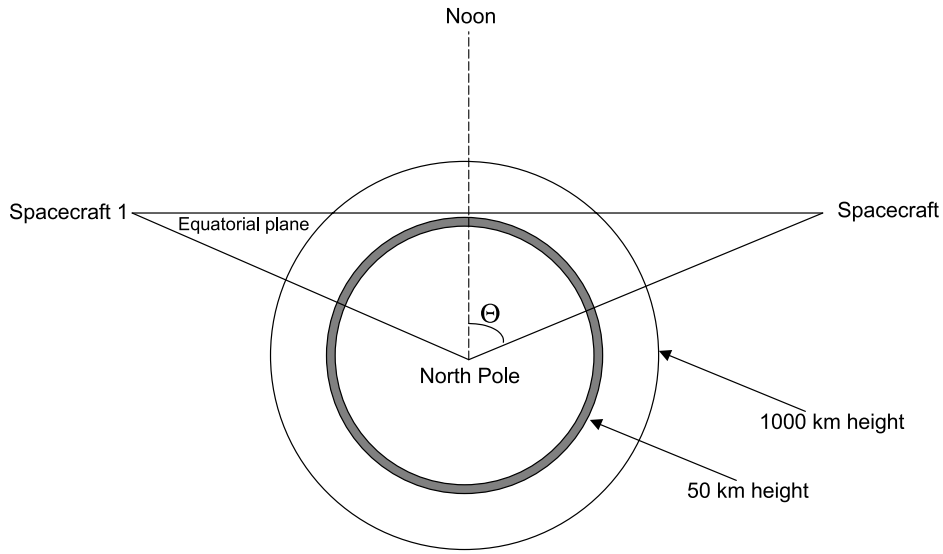

Figure 5. Geometry for a satellite-to-satellite communication. In order to make the figure clearer, the angle Θ represented here is larger than the 30° used in the computation.

[25] We have explored the degradation of the signal for active and quiet solar activity. For calm space weather conditions, the TEC between the 2 spacecraft is about 300 TECU. When it is stormy we have an integrated TEC between the 2 spacecraft of about 12 000 TECU. The results are computed taking the Faraday rotation into account. They are shown in Table 3.

[26] We see that the effect of the activity is to enhance the variation delay by about 43, the phase variation by about 42. However, the amplitudes of these variations remain negligible. The damping (i.e., 1, the amplitude variation) is more affected since it is multiplied by about 378. However, again, the amplitude is affected only by about 0.05%, which is negligible too.

5. Conclusion

[27] The new telecommunication developments require increasing precision in space to ground and in space to space communication. It becomes therefore necessary to explore numerically the influence of the thermospheric collisions on the different parameters of a propagating electromagnetic wave.

[28] We found that neither the ionosphere-thermosphere coupling nor the Faraday rotation can be considered as a possible error source for the GPS system for positioning purposes. In the case of TEC measurements, the effect of the thermosphere is negligible when the TEC is estimated by the ionospheric delay. There is no influence at all when the TEC is estimated by the Faraday rotation. Whatever the atmospheric conditions, this influence proves negligible. Indeed, even if the precision of our model does not allow in any manner to obtain exact values of these perturbations for given ionospheric parameters, we have worked out reliable orders of magnitudes.

[29] For satellite to ground communication, these influences remain negligible at lower frequencies down to the plasma frequency. The upper value of the delay variation is 10 cm at 10 MHz for satellite to ground communication. In the case of satellite-to-satellite communication, the variations are enhanced but still remain negligible.

Appendix A: Calculation of Refraction Index in a Collisionless Plasma

[30] This classical calculation has been proposed by Appleton-Hartree. We consider the plane wave approximation.

$$\vec{E}(\vec{r}) = \vec{E}_0 e^{j\left(\vec{k}\vec{r}-\omega_{GPS}t\right)} \tag{A1}$$

Table 3. Satellite-to-Satellite Communication: Variation of the delay, Phase, and Amplitude of the GPS Wave for Two Ionospheric Conditions

	Delay Variation, m	Phase Variation	Amplitude Variation
Quiet case	$0.61863446\ 10^{-7}$	$0.15907068\ 10^{-8}$	0.9999986644
Stormy case	$0.26438972\ 10^{-5}$	$0.67983043\ 10^{-7}$	0.9994939547

In our one-dimensional geometry, vectors become scalars:

$$E(r) = E_0 e^{j(kr-\omega_{GPS}t)}. \quad \text{(A2)}$$

In addition, applying the first momentum principle:

$$m_e \frac{d^2 r}{dt^2} = -eE, \quad \text{(A3)}$$

so we have:

$$V = \frac{dr}{dt} = \frac{-jeE(r,t)}{m_e \omega_{GPS}}. \quad \text{(A4)}$$

In a thermalized ionosphere, the ion velocity is negligible in front of the electron velocity. In this case, we can neglect the ions in the computation of the current density J:

$$J = -n_e(r)eV = n_e(r)e^2 \frac{j.E(r,t)}{m_e \omega_{GPS}}. \quad \text{(A5)}$$

We now consider the Maxwell equations:

$$\overrightarrow{rot}\left(\vec{E}\right) = -\frac{\partial \vec{B}}{\partial t}, \quad \text{(A6)}$$

$$\Leftrightarrow \overrightarrow{rot}\,\overrightarrow{rot}\left(\vec{E}\right) = -\frac{\partial\left(\overrightarrow{rot}\,\vec{B}\right)}{\partial t}, \quad \text{(A7)}$$

with Maxwell-Ampère:

$$\overrightarrow{rot}\left(\vec{B}\right) = \mu_0\left(\vec{J} + \varepsilon_0 \frac{\partial \vec{E}}{\partial t}\right). \quad \text{(A8)}$$

Injected in the previous equation, we have in one dimension:

$$\frac{\partial^2 E}{\partial r^2} + j\mu_0 \frac{n_e(r)e^2}{\omega_{GPS} m_e} \frac{\partial E}{\partial t} - \frac{1}{c^2}\frac{\partial^2 E}{\partial t^2} = 0. \quad \text{(A9)}$$

With the equation (A5) we obtain:

$$k^2 = \frac{\omega_{GPS}^2}{c^2} - \mu_0 \frac{n_e(r)e^2}{m_e}. \quad \text{(A10)}$$

Thus $k = \frac{\omega_{GPS}}{c}\sqrt{1 - \frac{\omega_P^2}{\omega_{GPS}^2}} = \frac{\omega_{GPS}}{c} N_r$ where N_r is the refractive index and ω_p is the plasma frequency:

$$\omega_P(r) = \sqrt{\frac{e^2 n_e(r)}{m_e \varepsilon_0}}. \quad \text{(A11)}$$

Therefore in the collisionless case:

$$N_r = \sqrt{1 - \frac{\omega_P^2}{\omega_{GPS}^2}}. \quad \text{(A12)}$$

Appendix B: Calculation of Refraction Index for a Collisional Plasma

[31] In the following, we neglect the rotation of the polarization plane, in order to put emphasis on the collision term in the refractive index. In the equation (A7) of the FDP we have to add a friction force due to electrons-neutrals collisions. Let us call ν the collision frequency. The characteristic time is $\tau = \frac{1}{\nu}$. The probability dp to have one collision during a time dt is:

$$p = \nu . e^{-\nu t} dt, \quad \text{(B1)}$$

but under a force F an electron moves on a distance $d = \frac{F\tau^2}{2m_e}$ during a time τ. The average motion of an electron between two collisions is then:

$$\overline{s} = \frac{F}{2m_e}\int_0^{+\infty} t^2 \nu e^{-\nu t} dt = \frac{F}{m_e \nu^2}. \quad \text{(B2)}$$

Thus, because there is ν collisions during 1 second, the velocity V is:

$$V = \frac{F}{m_e \nu}. \quad \text{(B3)}$$

In addition the friction force F is:

$$F = m_e \nu V. \quad \text{(B4)}$$

Now the first momentum equation becomes:

$$m_e \frac{d^2 r}{dt^2} = -e.E + m_e \nu \frac{dr}{dt}. \quad \text{(B5)}$$

Let us have $\vec{P}$ the polarization vector: $\vec{P} = n_e(r)e.\vec{r}$. Extracting r from this expression and deriving versus dt and dt^2, we obtain:

$$\frac{\partial r}{\partial t} = \frac{1}{n_e e}\frac{\partial P}{\partial t} = \frac{j\omega_{GPS} P}{n_e e} \quad \text{(B6)}$$

$$\frac{\partial^2 r}{\partial t^2} = \frac{\omega_{GPS}^2 P}{n_e e}, \quad \text{(B7)}$$

and equation (B5) becomes

$$P = \frac{\omega_{GPS}^2 \varepsilon_0}{\omega_{GPS}(j\nu - \omega_{GPS})} E. \quad \text{(B8)}$$

The refractive index N_r is expressed by:

$$N_r = \sqrt{\varepsilon_r} = \sqrt{1+\chi} \quad \text{and} \quad P = \varepsilon_0 \chi E. \tag{B9}$$

We extract the susceptibility χ as a function of the polarization, and inject its value (equation (B8) to retrieve the value of the refractive index in the collisional case:

$$N_r = \sqrt{1 - \frac{\omega_P^2}{\omega(\omega - j\nu)}}. \tag{B10}$$

Appendix C: Refractive Index Expansion and TEC Calculation

[32] Without collisions we have:

$$N_r = \sqrt{1 - \frac{\omega_P^2}{\omega_{GPS}^2}}. \tag{C1}$$

For $\omega_p \ll \omega_{GPS}$; we can expand n to the second order:

$$N_r = \left(1 - \frac{\omega_P^2}{2\omega_{GPS}^2}\right), \tag{C2}$$

with $\omega_P(r) = \sqrt{\frac{e^2 n_e(r)}{m_e \varepsilon_0}}$ we get:

$$N_r = 1 - \frac{e^2 n_e(r)}{8\pi^2 f^2 m_e \varepsilon_0}. \tag{C3}$$

Thus

$$\Delta R = \int_P^S (N_r - 1)dr = \int_P^S \frac{n_e(r)e^2}{8\pi\varepsilon_0 M f^2} \cdot dr = \frac{e^2}{8\pi^2\varepsilon_0 M f^2} \int_P^S n_e(r)dr. \tag{C4}$$

References

Bilitza, D. (2001), International Reference Ionosphere 2000, *Radio Sci.*, *36*, 261–276.

Brasseur, G., and S. Solomon (1984), *Aeronomy of Middle Atmosphere*, Springer, New York.

Delcourt, J. J. (2003), *Ionosphère*, Hermès Sci. Publ., Paris.

Hedin, A. E. (1991), Extension of the MSIS thermosphere model into the middle and lower atmosphere, *J. Geophys. Res.*, *96*, 1159–1172.

Huang, X., and B. W. Reinisch (1982), Automatic calculation of electron density profiles from digital ionograms: 2. True height inversion of topside ionograms with the profile-fitting method, *Radio Sci.*, *17*, 837–844.

Lilensten, J., and P. L. Blelly (2002), The TEC and F2 parameters as tracers of the ionosphere and thermosphere, *J. Atmos. Sol. Terr. Phys.*, *64*, 775–793.

Lilensten, J., and L. R. Cander (2003), Calibration of the TEC derived from GPS measurements and from ionospheric models using the EISCAT radar, *J. Atmos. Sol. Terr. Phys.*, *65*, 833–842.

Mannucci, A. J., B. D. Wilson, D. N. Yuan, C. H. Ho, U. J. Lindqwister, and T. F. Runge (1998), A global mapping technique for GPS-derived ionospheric total electron content measurements, *Radio Sci.*, *33*, 565–582.

Reinisch, B. W., and X. Huang (1982), Automatic calculation of electron density profiles from digital ionograms: 1. Automatic O and X trace identification for topside ionograms, *Radio Sci.*, *17*, 421–434.

Reinisch, B. W., and X. Huang (1983), Automatic calculation of electron density profiles from digital ionograms: 3. Processing of bottomside ionograms, *Radio Sci.*, *18*, 477–492.

Safaeinili, A., W. Kofman, J.-F. Nouvel, A. Herique, and R. L. Jordan (2003), Impact of Mars ionosphere on orbital radar sounder operation and data processing, *Planet. Space Sci.*, *51*, 505–515.

Schunk, R. W., and A. F. Nagy (2000), *Ionospheres*, Cambridge Univ. Press, New York.

Smith, F. L., III, and C. Smith (1972), Numerical evaluation of Chapman's grazing incidence integral ch (X,χ), *J. Geophys. Res.*, *77*, 3592–3597.

M. Barthélémy, P. Delorme, E. Engel, J. Lilensten, and S. Samouillan, Laboratoire de Planetologie de Grenoble, Batiment D de physique, B.P. 53, F-38041 Grenoble Cedex 9, France. (jean.lilensten@obs.ujf-grenoble.fr)